Available online at www.sciencedirect.com
ScienceDirect
Journal of Catalysis 245 (2007) 477–481
JOURNAL OF CATALYSIS
www.elsevier.com/locate/jcat

Research Note

A surfactant-assisted hydrothermal deposition method for preparing highly dispersed W/γ-Al_2O_3 hydrodenitrogenation catalyst

Yu Fan [a,b], Xiaojun Bao [a,b,*], Hao Wang [b], Chunfang Chen [b], Gang Shi [b]

[a] *State Key Laboratory of Heavy Oil Processing, China University of Petroleum, Beijing 102249, PR China*
[b] *The Key Laboratory of Catalysis, China National Petroleum Co. (CNPC), China University of Petroleum, Beijing 102249, PR China*

Received 24 July 2006; revised 21 October 2006; accepted 2 November 2006

Available online 1 December 2006

Abstract

Two W/γ-Al_2O_3 catalysts were prepared by a surfactant-assisted hydrothermal deposition method developed in the present investigation and the conventional impregnation method, respectively, and characterized by means of XRD, XPS, TEM, N_2 adsorptipn, NH_3-TPD and H_2-TPR. The results showed that compared with the catalyst prepared by impregnation, the catalyst prepared by the surfactant (cetyltrimethylammonium bromide, CTABr)-assisted hydrothermal deposition had higher dispersion of tungsten species with weak metal–support interaction, more open pore channels, and more acid sites, and thus presented a significantly enhanced hydrodenitrogenation activity. The novel method introduced here sheds a light on preparing supported metal catalysts with high activity.
© 2006 Elsevier Inc. All rights reserved.

Keywords: Surfactant-assisted hydrothermal deposition method; High dispersion; Weak metal–support interaction; Hydrodenitrogenation

1. Introduction

Hydrodenitrogenation (HDN) is one of the most important reactions performed during hydrotreating processes of petroleum-refining products [1]. It is widely accepted that the key points to prepare highly active HDN catalysts are the control of the structure and nature of the active sites [2,3]. One approach to achieving this goal is to use different support materials with high surface areas, such as activated carbons [4], mesoporous alumina [5], and mesoporous molecular sieves (e.g., MCM-41) [6]. Despite many promising laboratory results, these supports suffer from poor thermal/hydrothermal stability and thus are inapplicable to industry. Another approach is to increase the loading of active species while maintaining their high dispersion on support. However, further increasing the loading of active species by the conventional impregnation method yields limited improvement in catalyst HDN activity due to the increasing agglomeration tendency of the active species [7]. The equilibrium deposition filtration method reported by Karakonstantis et al. [8] could improve the dispersion of active species at high loadings, but this improvement results from the strong active phase–support interaction, which may limit its application due to the resulting incomplete sulfidation of active phases [9]. So far, there is no report on how to highly disperse active species on support without increasing the metal–support interaction. The present investigation addresses this issue.

Emerging as a powerful method for preparing various nanosized metal oxides [10], the hydrothermal deposition method (HDM) has gained wide application because of its capability to control the size, morphology, and surface chemistry of particles due to the unique hydrothermal conditions. It was noted that under the hydrothermal conditions, aqueous solutions also provide ions involved with high diffusivity and thus facilitate the deposition of nanoparticles on the internal surface of porous substrates [11]. These advantages of the HDM perfectly suit the requirements to highly disperse active metal species on porous supports; thus, the application of the HDM to the preparation of supported catalysts with higher metal loadings is expected to be an exciting approach to enhancing the activity of hydrotreating

* Corresponding author. Fax: +86 (0)10 8973 4979.
E-mail address: baoxj@cup.edu.cn (X. Bao).

0021-9517/$ – see front matter © 2006 Elsevier Inc. All rights reserved.
doi:10.1016/j.jcat.2006.11.003

catalysts. However, to the best of our knowledge, this approach has not yet been examined in the literature.

In this study, a highly dispersed W/γ-Al_2O_3 catalyst (designated as catalyst HD) was prepared by a surfactant (cetyltrimethylammonium bromide, CTABr)-assisted hydrothermal deposition method developed in the present investigation, and its acidity, its morphology, and the state of tungsten species were compared with those of a catalyst (denoted as catalyst IM) prepared by the conventional impregnation method. In addition, the HDN performance of the two catalysts was evaluated using 1.0 wt% pyridine in cyclohexane as a model compound.

2. Experimental

2.1. Catalyst preparation

Preparation of the oxidic catalyst HD involved the following steps. First, 6.0 g γ-Al_2O_3 particles (20–40 meshes, Sasol GmbH, Germany) were added into a 0.1 M sodium tungstate (99 wt%, Shantou Xilong Chemical Co., PR China) solution of 77.0 mL. Then, a 0.5 M ionic surfactant CTABr (99 wt%; Beijing Chemical Co., PR China) solution of 7.7 mL was slowly added to the above mixture and the dropwise addition of a 1 M HCl (37 wt%; Beijing Chemical Co., PR China) solution of 15.4 mL under stirring was followed. The resulting suspension was further stirred for 1 h and heated at 150 °C for 24 h after transferred to a 150-mL rotating Teflon-lined stainless steel autoclave. Finally, the resulting product was filtered, washed with deionized water, dried at 120 °C for 5 h, and calcined at 520 °C for 4 h.

Preparation of the oxidic catalyst IM involved the following steps. First, 6.0 g γ-Al_2O_3 particles were isometrically impregnated with an ammonium meta-tungstate (90 wt%; Ganzhou Qiandong Ltd., PR China) solution in proper proportion, and then the resulting product was aged at room temperature for 4 h, dried at 120 °C for 5 h, and calcined at 520 °C for 4 h.

The WO_3 content in the two calcined catalysts determined by X-ray fluorescence spectroscopy (XRF, ZSX-100e, Japan) was 23 wt%.

2.2. Characterization

X-ray diffraction (XRD) analyses were conducted on a Shimadzu 6000 diffractometer. X-ray photoelectron spectroscopy (XPS) analyses were conducted on a Shimadzu PHI-5300 ESCA spectrometer; all binding energies were calibrated using contaminant carbon (C_{1s} = 284.6 eV) as a reference. The transmission electron microscopy (TEM) images of the two calcined catalysts were obtained on a Philips Tecnai F-20 microscope. The surface area and pore volume measurements of the two calcined catalysts were conducted on a Micromeritics ASAP 2405N instrument at −195 °C using liquid N_2. Temperature-programmed reduction of hydrogen (H_2-TPR) and temperature-programmed desorption of ammonia (NH_3-TPD) were conducted on a home-built apparatus. The zeta potentials of alumina and tungstic acid were measured on a Malvern Zetasizer Nano ZS instrument, and the pH values of the solutions were measured on a Mettler-Toledo Delta 320 pH meter.

2.3. Catalytic activity assessment

After the catalysts were presulfurized in situ by a 10% H_2S/H_2 mixture at 400 °C and 3.0 MPa, the HDN reactions of the model compound 1.0 wt% pyridine in cyclohexane were carried out in a fixed-bed microreactor loaded with 3.0 g catalyst under the following conditions: 340 °C, volume hourly space velocity of the model compound of 1.0 h^{-1}, total pressure of 3.0 MPa, and volumetric ratio of H_2 to the model compound of 350. After the steady state was reached, the products were collected and analyzed by an Agilent 1790 gas chromatograph equipped with a flame ionization detector and a capillary column (50 m × 0.2 mm). The HDN activities of the catalysts were calculated in terms of pyridine conversion.

3. Results and discussion

3.1. XRD and XPS

The XRD patterns of the calcined catalysts are shown in Fig. 1. The peaks at $2\theta = 37.4°$, 45.9°, and 67.1° are attributed to the pure γ-Al_2O_3 phase, and those at $2\theta = 23.1°$, 23.6°, and 24.4° are assigned to the bulk WO_3 crystallites formed due to the higher loading of WO_3 compared with its dispersion capacity on alumina [8]. Obviously, there exists a characteristic triplet of the bulk WO_3 crystallite in the pattern of the oxidic catalyst IM, whereas it disappears in the pattern of the oxidic catalyst HD. These results reveal that the WO_3 particles in the oxidic catalyst HD are too small to be detected, as further confirmed by the TEM results shown in Fig. 2.

Lee et al. [12] stated that the XPS intensity ratios of the metal cations in the supported metal oxide to those in the oxide support can provide the important information regarding the dispersion and crystallite size of supported particles. Thus, the W_{4f}/Al_{2p} intensity ratios on the two oxidic catalysts were calculated; the results are given in Table 1. It can be seen that the

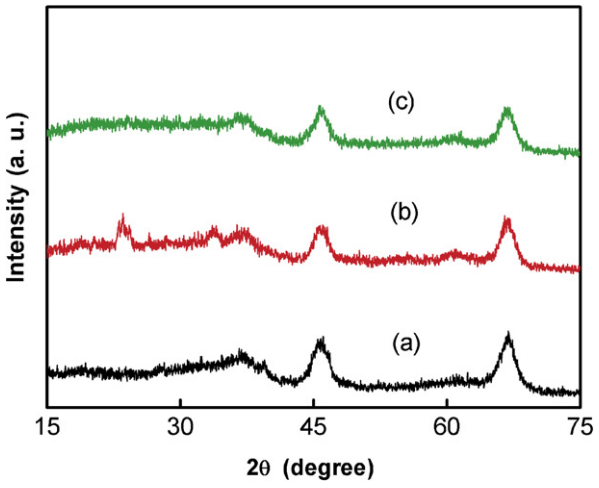

Fig. 1. XRD patterns of (a) γ-Al_2O_3, (b) oxidic catalyst IM, and (c) oxidic catalyst HD.

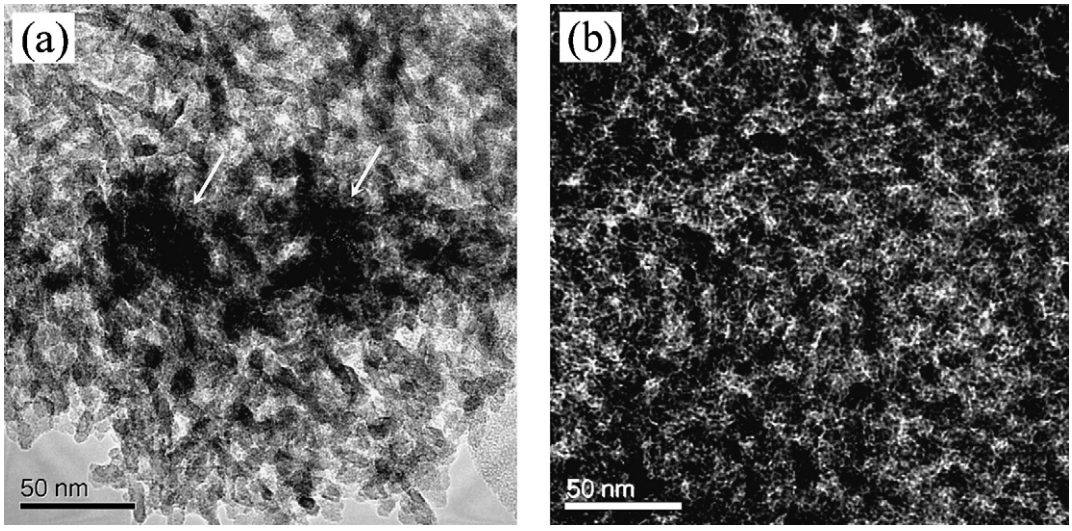

Fig. 2. TEM images of (a) oxidic catalyst IM and (b) oxidic catalyst HD.

Table 1
Typical properties of the two oxidic catalysts

	Surface W_{4f}/Al_{2p} ratio[a]	Surface area[b] (m^2/g)	Pore volume[b] (cm^3/g)	Acidity[c] ($\mu mol\ NH_3/g_{cat}$)	Maximum NH_3 desorption temperature[c] (°C)
γ-Al_2O_3	–	210	0.49	–	–
Catalyst IM	0.058	184	0.38	291	150
Catalyst HD	0.106	203	0.44	358	156

[a] Obtained by comparing the peak area of the W_{4f} region with that of the Al_{2p} region in XPS spectra.
[b] Obtained by N_2 adsorption.
[c] Obtained by NH_3-TPD.

ratio for the oxidic catalyst HD is 0.106, 1.8 times of that for the oxidic catalyst IM, even though their WO_3 contents, as determined by XRF, are the same, indicating that the HDM can greatly improve the dispersion of WO_3 on γ-Al_2O_3 and thus generate more active sites on the support surface.

3.2. TEM and N_2 adsorption

The morphologies of the two oxidic catalysts shown in Fig. 2 demonstrate that the WO_3 particles on the oxidic catalyst IM (confirmed by the energy-dispersive X-ray spectroscopy) obviously exist in the form of aggregates with an average size of ca. 40 nm, as pointed out by the white arrows, whereas those on the oxidic catalyst HD have an average size of ca. 14 nm, suggesting the effectiveness of the HDM in increasing the dispersion of the active species because the size of the supported particles can be considered an index representing dispersion [13].

The pore structure data of the two oxidic catalysts listed in Table 1 indicate that although both catalysts have lower surface areas and pore volumes than the support γ-Al_2O_3, the oxidic catalyst IM has much larger decreases in its surface area and pore volume due to the formation of the larger WO_3 particles, which may cause partial closing of the narrower pores of the support [14], in concordance with the above TEM analysis results.

3.3. NH_3-TPD

The acidity measurement results of the two oxidic catalysts given in Table 1 show that the maximum desorption temperatures of ammonia on the oxidic catalysts IM and HD are 150 and 156 °C, respectively, indicating the slightly higher acid strength of the oxidic catalyst HD compared with the oxidic catalyst IM [15]. Table 1 also shows that the oxidic catalyst HD has a higher acid quantity than the oxidic catalyst IM, because WO_3 has Lewis acid sites [16]. The acidity difference between the two catalysts with the same loading of WO_3 should be ascribed to the different exposure degrees of WO_3 derived from the two different preparation methods.

3.4. H_2-TPR

The H_2-TPR profiles given in Fig. 3 show that on the two curves, there is a steady increase in the baseline in the temperature range of 200–800 °C, followed by a well-developed large peak with its center at 981 °C for the oxidic catalyst HD or at 1016 °C for the oxidic catalyst IM. The lower maximum reduction temperature of the oxidic catalyst HD by 35 °C than that of the oxidic catalyst IM can be ascribed to the weaker interaction between the tungsten oxide species and the alumina support, as demonstrated by Kim et al. [17].

The XRD, XPS, TEM, and N_2 adsorption results confirm that tungsten oxide can be highly dispersed on alumina by the

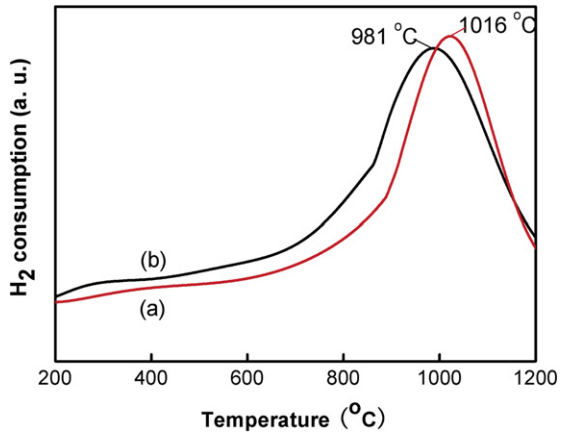

Fig. 3. H_2-TPR profiles of (a) oxidic catalyst IM and (b) oxidic catalyst HD.

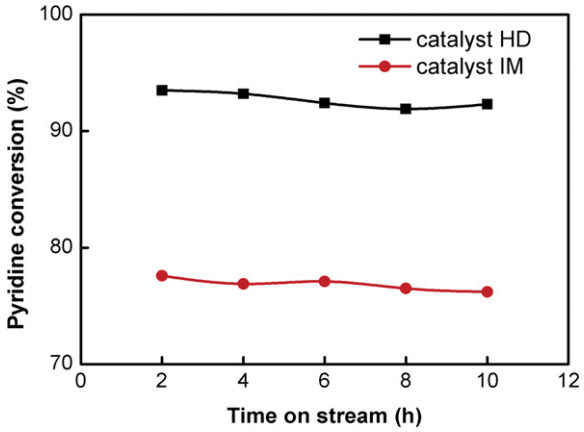

Fig. 4. HDN activities of the two W/γ-Al_2O_3 catalysts.

HDM. It is interesting to note that different from the widely accepted concept that the higher dispersion of active species on a catalyst support results from the stronger active species–support interaction [14], the H_2-TPR results obtained in this study demonstrate that the HDM can produce catalyst with higher dispersion of the active species but with weaker active species–support interaction. This interesting phenomenon may be explained as follows. On one hand, the electrophoresis measurement results show that the zeta potential of alumina is 37.9 mV and that of the tungstic acid nanoparticles formed via the reaction between HCl and Na_2WO_4 is −44.2 mV under the preparation conditions; thus, the electropositive alumina surface can easily adsorb the electronegative tungstic acid nanoparticles by the strong charge interaction, similar to the metal–support interaction that occurs during the impregnation process. However, the charge interaction can be greatly restrained with the introduction of the surfactant CTABr into the preparation solution because the uniformly distributed CTA^+ cations from electroionization of CTABr can preferentially interact with the electronegative tungstic acid nanoparticles. On the other hand, the carbonaceous species formed by the decomposition of the surfactant CTABr during the calcination can prevent sintering of tungsten oxide nanoparticles [18]. On the whole, the surfactant CTABr acts as a textural stabilizer for highly dispersing tungsten species on the alumina surface. Further study of the mechanism of the HDM by the spectroscopic method is under consideration.

3.5. Catalytic activity assessment

The HDN activities of the two W/γ-Al_2O_3 catalysts are shown in Fig. 4. Compared with the sulfided catalyst IM, the sulfided catalyst HD presents much higher HDN activity, giving an increase of 16% in pyridine conversion. Because the characterization results for the oxidic catalysts, especially considering the dispersion of the supported phases, also hold for the final sulfided catalysts [19], the difference between the HDN activities of the two sulfided catalysts can be explained as follows. On one hand, as mentioned above, the catalyst HD has the better dispersed tungsten species and more acid sites than the catalyst IM, which are favorable for the HDN of pyridine [20]; on the other hand, the strong interaction between tungsten oxide and alumina on the catalyst IM prepared by impregnation may result in the inadequate sulfurization of WO_3 species deposited, thus leading to poor catalyst activity [9], whereas the WO_3 species on the catalyst HD can be fully sulfurized because of the weakened interaction, and thus more WS_2 active sites can be generated. In summary, the HDM introduced here provides the catalyst with higher dispersion of the active tungsten species and weaker metal–support interaction, both of which ensure good HDN activity of the resulting catalyst.

4. Conclusions

Significantly different from various methods for improving the dispersion of active metal species by strengthening the metal–support interaction, the surfactant-assisted hydrothermal deposition method developed in the present investigation could realize the higher dispersion of active metal species while yielding the weaker metal–support interaction via the adjusting and stabilizing effects of the surfactant CTABr on the structure of active species. Compared with the catalyst prepared by impregnation, the as-prepared W/γ-Al_2O_3 catalyst with the same composition showed greatly improved HDN activity, endowing this novel method with great potential for enhancing the catalytic activity of supported metal catalysts.

Acknowledgments

This work was supported by the National Basic Research Program of China (Grant 2004CB217807), the Natural Science Foundation of China (Grant 20606037), and the CNPC Innovation Foundation (Grant 05E7020).

References

[1] P. Grange, Catal. Rev. Sci. Eng. 21 (1980) 135.
[2] R. Prins, Adv. Catal. 46 (2001) 399.
[3] E. Furimsky, F.E. Massoth, Catal. Rev. Sci. Eng. 47 (2005) 297.
[4] A.F. Pérez-Cadenas, F.J. Maldonado-Hódar, J.L.G. Fierro, C. Moreno-Castilla, J. Phys. Chem. B 107 (2003) 4997.

[5] L. Kaluža, M. Zdražil, N. Žilková, J. Čejka, Catal. Commun. 3 (2002) 151.
[6] A. Wang, L. Ruan, Y. Teng, X. Li, M. Lu, J. Ren, Y. Wang, Y. Hu, J. Catal. 229 (2005) 314.
[7] F. Patcas, W. Krysmann, D. Honicke, F.C. Buciuman, Catal. Today 69 (2001) 379.
[8] L. Karakonstantis, H. Matralis, Ch. Kordulis, A. Lycourghiotis, J. Catal. 162 (1996) 306.
[9] M.J. Vissenberg, Y. van der Meer, E.J.M. Hensen, V.H.J. de Beer, A.M. van der Kraan, R.A. van Santen, J.A.R. van Veen, J. Catal. 198 (2001) 151.
[10] B.B. Lakshmi, P.K. Dorhout, C.R. Martin, Chem. Mater. 9 (1997) 857.
[11] M. Kang, S.J. Choung, J.Y. Park, Catal. Today 87 (2003) 87.
[12] J.J. Lee, H. Kim, J.H. Koh, A. Jo, S.H. Moon, Appl. Catal. B 58 (2005) 89.
[13] G. de la Puente, A. Gil, J.J. Pis, P. Grange, Langmuir 15 (1999) 5800.
[14] Ch. Papadopoulou, J. Vakros, H.K. Matralis, G.A. Voyiatzis, Ch. Kordulis, J. Colloid Interface Sci. 274 (2004) 159.
[15] F. Arena, R. Dario, A. Parmaliana, Appl. Catal. A 170 (1998) 127.
[16] C. Martin, P. Malet, G. Solana, V. Rives, J. Phys. Chem. B 102 (1998) 2759.
[17] C.H. Kim, W.L. Yoon, I.C. Lee, S.I. Woo, Appl. Catal. A 144 (1996) 159.
[18] P. Afanasiev, G. Xia, G. Berhault, B. Jouguet, M. Lacroix, Chem. Mater. 11 (1999) 3216.
[19] S. Dzwigaj, C. Louis, M. Breysse, M. Cattenot, V. Bellière, C. Geantet, M. Vrinat, P. Blanchard, E. Payen, S. Inoue, H. Kudo, Y. Yoshimura, Appl. Catal. B 41 (2003) 181.
[20] Y.C. Park, E.S. Oh, H.K. Rhee, Ind. Eng. Chem. Res. 36 (1997) 5083.